*Regular Paper*

# Homography from Conic Intersection: Camera Calibration based on Arbitrary Circular Patterns

HAIYUAN WU ,† QIAN CHEN † and TOSHIKAZU WADA†

For the camera calibration, point correspondence data between 3D and 2D points widely spreading over the image plane is necessary to get a precise result. However, in the case of wide observing area, it is impractical to use a huge calibration object that covers the camera view. This paper presents a refined calibration method using circular patterns. We already proposed a circular pattern based camera calibration method using a four-wheel mobile robot. That is, by keeping low speed and constant steering angle, the robot can draw a big circular pattern on a plane. Our previous method, however, has a limitation that roll angle around the optical axis is assumed to be zero. This paper presents an improved version of the camera calibration method. Our method estimates the extrinsic parameters of fixed camera from a single circular trajectory when the focal length of the camera is known. In the case that the focal length is not given, two co-planar un-concentric circular trajectories are enough for calibrating the extrinsic parameters and the focal length. In both cases, the center and the radius of the circle(s), the speed of the robot are not required. The extensive experiments over simulated images as well as real images demonstrate the robustness and the accuracy of our method.

## 1. Introduction

Camera calibration plays an important role for Computer Vision tasks, e.g., stereo vision, volume intersection, generating an orthogonal view of a planar scene from a perspective view, and so on.

For calibrating the extrinsic camera parameters, point correspondence data between known 3D points and their projection is necessary. In many cases, specially designed calibration objects are employed for the ease of this point correspondence. In order to get precise camera parameters, point correspondence data between 3D and 2D points spreading over the image plane is necessary. This implies the calibration object should be big enough for covering the camera view. This requirement can be satisfied in the indoor scenes. However, it is impractical for the wide observing area, such as, a baseball stadium or a football playground, to construct a huge calibration object that covers the camera view. Furthermore, using calibration objects is not suitable for the automatic calibration, because points on the objects are manually corresponded in many cases. The manual correspondence sometimes produces erroneous data.

This paper presents a method for solving the above problems, i.e., an automatic camera calibration method that can be used for estimating extrinsic parameters of a fixed camera between the camera and a far planar object, such as, floors, roads, playgrounds, and so on.

**Basic Idea:** In this research, we employ a four-wheel radio controlled car (hereafter "*RC car*") moving on a plane as a calibration object. Although the RC car cannot move along a straight line without a navigation system, it is easy to drive it along a circular trajectory by keeping low speed and constant steering angle. The circular trajectory is projected as an ellipse on to the image plane (Figure 1). Based on this geometric property, we developed a refined method for camera calibration using circular patterns.


**Fig. 1** The addressed problem: calibrating extrinsic camera parameters using four-wheel mobile robot

Our method estimates the extrinsic parameters of fixed camera from a single circular trajectory when the focal length of the camera is known. In the case that the focal length is not given, two co-planar un-concentric circular trajectories are enough for calibrating the extrinsic parameters and the focal

† Wakayama University

length. In both cases, our method does not require the point correspondence data, the center position and the radius of the circular trajectory. In addition, it does not require the speed of the robot to be known, and the completely circular trajectory to be seen. Through computer simulations and experiments with some real images, we confirmed that our method is robust and accurate. We also confirmed that our method gives higher accuracy than the homography based algorithm.

**Related Work:** Several camera calibration methods using circular patterns[2)-5)], or conics[6)-10)] have been proposed so far. Most of them assume multi-viewpoint images. Meng *et al.*[2)] proposed a method that uses a planar circle and lines passing through its center. It requires at least three different views. Kim *et al.*[4)] proposed a method that makes use of planar con-centric circles. It requires two views. Yang *et al.*[5)] proposed a similar method like Kim's one except that con-centric ellipses are used instead of con-centric circles. Avidan *et al.*[7)] proposed an approach to reconstructing the 3D coordinates of a moving point along a conic section viewed by a monocular moving camera. It requires nine views. If the point is known to move along a circle, it needs seven views.

We have proposed a camera calibration method using a single circular pattern[14)]. However, It has a limitation that roll angle around the optical axis is assumed to be zero.

Homography can be used as a camera calibration method using a planar pattern. It requires at least four point correspondences to estimate the matrix that convert points on an image plane to the corresponding points on another image plane. By decomposing the homography matrix, we can estimate the surface normal vector of the plane, the translation, and the rotation between the two cameras. But the decomposition is alternative[12)13)].

The addressed problem in this paper is to estimate the extrinsic camera parameters from one image containing circular pattern(s) on a plane. The extrinsic parameters consist of 1) translation vector $\mathbf{T}$ from the center of a circle to the viewpoint, and 2) rotation matrix $\mathbf{R}$ that transforms the viewpoint to an orthogonal viewpoint where the perspective projection of the plane can be represented by a scaling, as shown in Figure 2. In the case that the focal length of the camera is unknown, its estimation is also our target.

## 2. Calibration from circular patterns

From a generic viewpoint, a circle is observed as an ellipse on the image plane by perspective projection. As shown in figure 3, a ray passing through the observed ellipse and the viewpoint forms an oblique elliptical cone. In addition, the ray passing through the base circle and the viewpoint forms an oblique circular cone. It is clear that the oblique elliptical cone and the oblique circular cone denote the same cone. The difference between them is base planes, where the ellipse base and the circle base reside on.

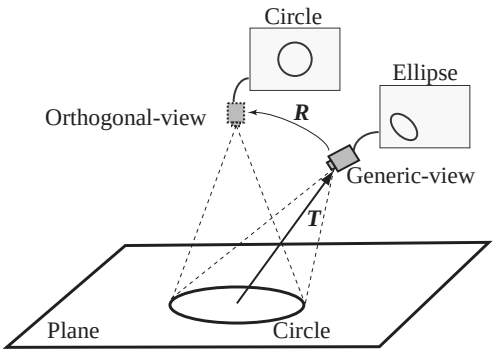


**Fig. 2** Observing a circle from a generic viewpoint and from an orthogonal viewpoint, $\mathbf{R}$ and $\mathbf{T}$ are the rotation matrix and the translation vector of the camera

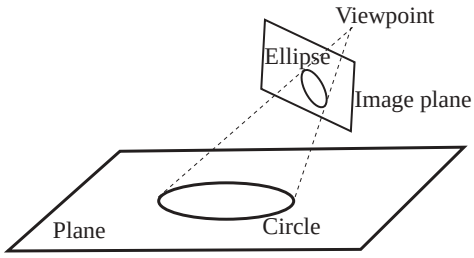


**Fig. 3** A circle and its projection

The $\mathbf{R}$ represents the rotation between the image plane and planes parallel to the base plane where circular pattern(s) reside on. So, the $\mathbf{R}$ can be estimated by finding the rotation that converts the oblique elliptical cone defined by the viewpoint and the observed ellipse to an oblique circular cone. Then, our problem ends up estimating this rotation transform. Once the $\mathbf{R}$ is estimated, the $\mathbf{T}$ can easily be estimated except the scale factor. That is, the direction of $\mathbf{T}$ can be determined.

In the case that the focal length of the camera is unknown, two un-concentric circular patterns on the same plane are required for calibration. By assuming a focal length $f$, we can suppose two oblique elliptical cones, and estimate two $\mathbf{R}$s. If the difference between the estimated $\mathbf{R}$s is minimized, the assumed focal length should be regarded as a valid estimation.

### 2.1 Oblique elliptical cones and oblique circular cones

Here we describe a method to compute a rotation matrix that transforms an oblique elliptical cone to an oblique circular cone. The method consists of two steps. First, we compute a rotation matrix that transforms an oblique elliptical cone to an (un-oblique) elliptical cone. Then we compute another rotation matrix that transforms the (un-oblique) elliptical cone to an oblique circular cone.

#### 2.1.1 Oblique elliptic cones

Here we explore a relation between an ellipse on $z = z_0$ plane and an oblique elliptical cone defined by the ellipse and an apex at the origin (Figure 4).

An ellipse on $z = z_0$ plane can be represented by

$$Ax^2+2Bxy+Cy^2+2Dx+2Ey+F = 0. \quad (1)$$

Eq.(1) can be rewritten in quadratic form as

$$\mathbf{X}^T\mathbf{Q}\mathbf{X} = 0, \quad (2)$$

where

$$\mathbf{Q} = \begin{bmatrix} A & B & D \\ B & C & E \\ D & E & F \end{bmatrix}, \quad \mathbf{X} = \begin{bmatrix} x \\ y \\ 1 \end{bmatrix} \quad (3)$$

Let $\mathbf{X_e} = [x \;\; y \;\; z_0]^T$ be a point on a 3D ellipse given by Eq.(2) on $z = z_0$ plane, then the following equation stands:

$$\mathbf{X} = \mathbf{K}\mathbf{X_e}, \quad (4)$$

where $\mathbf{K} = diag(1, 1, 1/z_0)$. By substituting Eq.(4) for $\mathbf{X}$ in Eq.(2), we obtain

$$\mathbf{X}^T\mathbf{Q}\mathbf{X} = \mathbf{X_e}^T\mathbf{Q_e}\mathbf{X_e} = 0, \quad (5)$$

where

$$\mathbf{Q_e} = \mathbf{K}\mathbf{Q}\mathbf{K}. \quad (6)$$

That is, $\mathbf{Q_e}$ characterizes the 3D ellipse on $z = z_0$ plane.

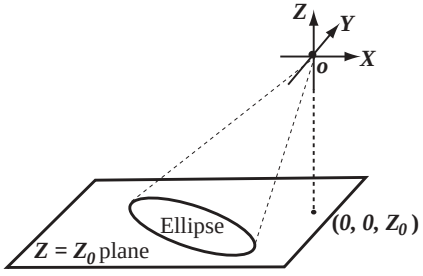


**Fig. 4** An oblique elliptical cone formed from an ellipse

Let $\mathbf{P}$ be a point on a line segment connecting the origin $[0 \;\; 0 \;\; 0]^T$ and $\mathbf{X_e}$ on the 3D ellipse. $\mathbf{P}$ can be expressed by

$$\mathbf{P} = h\mathbf{X_e}. \quad (7)$$

where $h$ is a height parameter, i.e., $h = 0$ at the origin, and $h = 1$ at $z = z_0$. By substituting $\mathbf{P}$ for $\mathbf{X_e}$ in Eq.(5), we obtain the following equation:

$$\mathbf{P}^T\mathbf{Q_e}\mathbf{P} = h^2(\mathbf{X_e}^T\mathbf{Q_e}\mathbf{X_e}) = 0. \quad (8)$$

Eq.(8) shows that the oblique elliptical cone and the 3D ellipse are represented by the same quadratic form $\mathbf{X}^T\mathbf{Q_e}\mathbf{X}$.

Circles and oblique circular cones are the special cases of ellipses and oblique elliptical cones. Suppose a 3D circle centered at $(x_0, y_0, z_0)$ on $z = z_0$ plane with radius $r$. The quadratic form of the following matrix represents the oblique circular cone defined by the 3D circle and an apex at the origin:

$$\mathbf{Q_c} = \begin{bmatrix} 1 & 0 & -\frac{x_0}{z_0} \\ 0 & 1 & -\frac{y_0}{z_0} \\ -\frac{x_0}{z_0} & -\frac{y_0}{z_0} & \frac{x_0^2+y_0^2-r^2}{z_0^2} \end{bmatrix}. \quad (9)$$

#### 2.1.2 Converting an oblique elliptical cone to an elliptical cone

In order to compute the rotation matrix that transforms an oblique elliptical cone to an oblique circular cone, we first compute the matrix that transforms the oblique elliptical cone to an (un-oblique) elliptical cone (Figure 5).

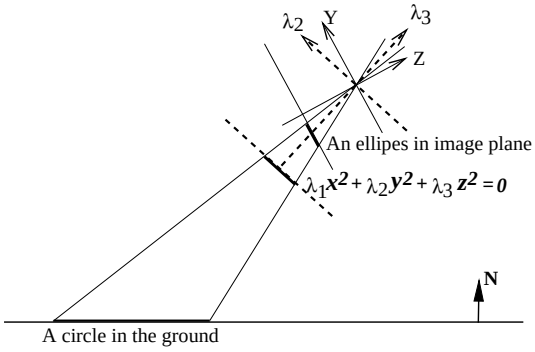


**Fig. 5** The oblique elliptical cone to an elliptical cone

An un-oblique elliptical cone in standard form is given by

$$\frac{x^2}{a^2} + \frac{y^2}{b^2} = z^2. \quad (10)$$

Eq.(8) describes that an oblique elliptical cone is represented by a quadratic form of $\mathbf{Q_e}$. Thus $\mathbf{Q_e}$ have 3 real eigenvalues $\lambda_1$, $\lambda_2$, and $\lambda_3$ satisfying:

$$\lambda_1\lambda_2\lambda_3 < 0. \quad (11)$$

Without losing generality, we assume that

$$\lambda_1\lambda_2 > 0, \quad |\lambda_1| \geq |\lambda_2| \;. \quad (12)$$

Let $\mathbf{v_1}$, $\mathbf{v_2}$ and $\mathbf{v_3} = \mathbf{v_1} \times \mathbf{v_2}$ be the normalized eigenvectors corresponding to $\lambda_1$, $\lambda_2$ and $\lambda_3$, respectively. Using the eigenvalues and eigenvectors, $\mathbf{Q_e}$ can be decomposed as

$$\mathbf{Q_e} = \mathbf{V}\mathbf{\Lambda}\mathbf{V}^{-1} = \mathbf{V}\mathbf{\Lambda}\mathbf{V}^T, \quad (13)$$

where

$$\begin{array}{ll}\mathbf{\Lambda} & = diag(\lambda_1, \lambda_2, \lambda_3) \\ \mathbf{V} & = \left[ \begin{array}{ccc} \mathbf{v_1} & \mathbf{v_2} & \mathbf{v_3} \end{array} \right] \end{array} .$$

By rotating the oblique elliptical cone with $\mathbf{V}^T$, we obtain

$$\begin{array}{ll}\mathbf{P}^T\mathbf{Q_e}\mathbf{P} & = (\mathbf{VP'})^T(\mathbf{V\Lambda V}^{-1})(\mathbf{VP'}) \\ & = \mathbf{P'}^T\mathbf{\Lambda P'} = 0 \end{array} , (14)$$

where $\mathbf{P'} = \mathbf{V}^T\mathbf{P}$.

Thus, the oblique elliptical cone can be expressed in the normalized form as following:

$$\lambda_1 x'^2 + \lambda_2 y'^2 + \lambda_3 z'^2 = 0. \quad (15)$$

By comparing Eq.(10) with Eq.(15), we can estimate the values $a$ and $b$ as follows:

$$\left\{ \begin{array}{ll} a & = \sqrt{-\lambda_3/\lambda_1} \\ b & = \sqrt{-\lambda_3/\lambda_2} \end{array} \right. . \quad (16)$$

From Eq.(12) we obtain $0 < a \leq b$.

### 2.1.3 Converting an elliptical cone to an oblique circular cone

Our problem is to compute the rotation matrix $\mathbf{U}$ that transforms an elliptical cone expressed by Eq.(10) to an oblique circular cone expressed by Eq.(9).(See figure 6)

This problem can be formalized by the following equation:

$$\mathbf{U}^T diag(1/a^2, 1/b^2, -1)\mathbf{U} = k\mathbf{Q_c}. \quad (17)$$

Since $\mathbf{U}$ is a rotation matrix, it can be represented by three orthogonal unit vectors: $\mathbf{U} = [\mathbf{u_1}\ \mathbf{u_2}\ \mathbf{u_3}]$, where $\mathbf{u_i} = [u_{ix}\ \ u_{iy}\ \ u_{iz}]^T; (i = 1, 2, 3)$. We also have

$$\mathbf{U}^T\mathbf{U} = \mathbf{I}. \quad (18)$$

From Eq.(17) we obtain

$$\left\{ \begin{array}{ll} \frac{a^2+1}{a^2}u_{1x}^2 + \frac{b^2+1}{b^2}u_{1y}^2 & \\ \quad -\frac{a^2+1}{a^2}u_{2x}^2 - \frac{b^2+1}{b^2}u_{2y}^2 & = 0 \\ \frac{a^2+1}{a^2}u_{1x}u_{2x} + \frac{b^2+1}{b^2}u_{1y}u_{2y} & = 0 \end{array} \right. . (19)$$

By simplifying Eqs.(18) and (19), we obtain

$$\begin{array}{ll} \mathbf{u_1} & = \left[ \begin{array}{c} \delta\cos\alpha \\ \sin\alpha \\ (-1)^{l-m}\sqrt{1-\delta^2}\cos\alpha \end{array} \right] \\ \mathbf{u_2} & = \left[ \begin{array}{c} (-1)^m\delta\sin\alpha \\ -(-1)^m\cos\alpha \\ (-1)^l\sqrt{1-\delta^2}\sin\alpha \end{array} \right] \\ \mathbf{u_3} & = \left[ \begin{array}{c} (-1)^l\sqrt{1-\delta^2} \\ 0 \\ -(-1)^m\delta \end{array} \right] \end{array} , (20)$$

where

$$\delta = \sqrt{\frac{1+1/b^2}{1+1/a^2}}, \quad (21)$$

and $\alpha$ is a free variable, $l$ and $m$ are arbitrary integer number. $\mathbf{u_1}$, $\mathbf{u_2}$ and $\mathbf{u_3}$ are the unit vectors of $X$, $Y$ and $Z$ axes of the coordinates system that describes the oblique circular cone. Thus $\mathbf{u_3}$ is the normal vector of the base plane of the oblique circular cone. From Eq.(20) we notice that there are four possible solutions of $\mathbf{u_3}$. Since $\mathbf{u_3}$ and $-\mathbf{u_3}$ describe the two normal vectors of the same plane, the number of meaningfully different solutions is two.

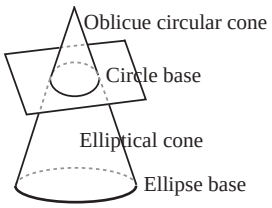


**Fig. 6** Convert an elliptical cone to an oblique circular cone

By substituting Eq.(20) for $\mathbf{U}$ in Eq.(17), we can compute the values of $x_0/z_0$, $y_0/z_0$ and $r/z_0$. Then we transform $(x_0/z_0, y_0/z_0, 1)$ back to the coordinates system that describes the elliptical cone with $\mathbf{U}^T$ to compute the center $\mathbf{C_0}$ and the radius $r$ of the circular base as following:

$$\begin{array}{ll} \mathbf{C}_0 & = \left[ \begin{array}{c} -(-1)^l\sqrt{\frac{b^2-a^2}{1+a^2}}bz_0 \\ 0 \\ (-1)^m\sqrt{\frac{1+b^2}{1+a^2}}\frac{b}{a}z_0 \end{array} \right] , \quad (22) \\ r & = \frac{b^2}{a}|z_0| \end{array}$$

where $z_0$ remains as a scale factor that describes the distance between the origin and the plane where the circular base resides on.

In consequence, the rotation matrix $\mathbf{R}$ that transforms an oblique elliptical cone to an oblique circular cone is obtained by $\mathbf{R} = \mathbf{UV}$.

## 2.2 Calibration with known focal length

Here, we describe a method to estimate the extrinsic parameters of fixed camera by using one circular pattern.

In this paper, we assume a pinhole camera model and will use two coordinates systems as shown in Figure 7: 1) the world coordinates system ($O$-$XYZ$), and 2) camera coordinates system ($O'$-$X'Y'Z'$). The origins of both coordinates systems are set at the projection center of the camera. The $Z$-axis of $O$-$XYZ$ is set to be parallel to the normal vector of the ground. The $Z'$-axis of $O'$-$X'Y'Z'$ is set to be parallel to the optical-axis of the camera. The $Y$-axis of $O$-$XYZ$ is set to be perpendicular to $Z$-axis and $Z'$-axis.

The scene configuration is characterized by the following parameters: 1) the distance between the base plane (ground) and the viewpoint (projection center) $z_g$; 2) the radius of the circle $r$; 3) the focal

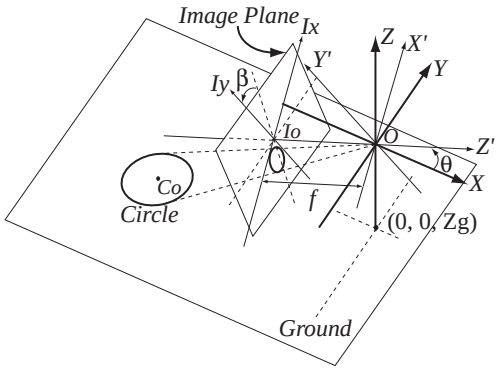


**Fig. 7** The world coordinate systems and the camera coordinate system

length $f$, i.e., the distance between the projection center and the image plane.

The parameters to be estimated are 1) the tilt angle $\theta$ between the $X$-axis and the $Z'$-axis; 2) the roll angle $\beta$ between the $Y$-axis and $X'$-axis; 3) the translation vector $\mathbf{T}$ that describes the center of the circle $\mathbf{C_0}$ in $O'$-$X'Y'Z'$ coordinates system.

By observing a circle on a plane, such as ground, we have an image where the circle shows an ellipse. Let $\mathbf{Q}$ is the ellipse detected from the image. We define an oblique elliptical cone whose apex is at the projection center and the base is the ellipse on the image plane. From Eq.(5), we obtain a quadratic form matrix $\mathbf{Q_e}(f)$ that describes the oblique elliptical cone as following:

$$\mathbf{Q_e}(f) = \mathbf{K}(f)^T\mathbf{Q}\mathbf{K}(f) = \mathbf{K}(f)\mathbf{Q}\mathbf{K}(f), \quad (23)$$

where $\mathbf{K}(f) = diag(1, 1, -1/f)$. Because $\mathbf{K}(f)$ is a function of $f$, then $\mathbf{Q_e}(f)$ is also a function of $f$.

With the method described in **2.1.2**, we can compute the rotational matrix $\mathbf{V}(f)$ that transforms the oblique ellipse cone $\mathbf{Q_e}$ to an ellipse cone expressed by Eq.(10) by computing the eigenvalues and the eigenvectors of $\mathbf{Q_e}$:

$$\mathbf{V}(f) = \left[ \begin{array}{ccc} \mathbf{v_1}(f) & \mathbf{v_2}(f) & \mathbf{v_3}(f) \end{array} \right], \quad (24)$$

$$\left\{ \begin{array}{ll} a(f) & = \sqrt{-\lambda_3(f)/\lambda_1(f)} \\ b(f) & = \sqrt{-\lambda_3(f)/\lambda_2(f)} \end{array} \right. , \quad (25)$$

where $\mathbf{V}(f)$, $a(f)$ and $b(f)$ are also functions of $f$.

With the method described in **2.1.3**, we estimate the unit vector of $Z$-axis that is the normal vector of the ground where the circle resides on by computing the rotation matrix $\mathbf{U}(f)$ that transforms the elliptic cone to an oblique circular cone. By substituting Eq.(21) for $\delta$ in Eq.(20), we obtain:

$$\mathbf{u_3}(f) = \left[ \begin{array}{c} (-1)^l\sqrt{\frac{1/a(f)^2 - 1/b(f)^2}{1+1/a(f)^2}} \\ 0 \\ -(-1)^m\sqrt{\frac{1+1/b(f)^2}{1+1/a(f)^2}} \end{array} \right]. \quad (26)$$

The representation of unit vector of the $Z$-axis $\mathbf{N}(f)$ under $O'$-$X'Y'Z'$ can be obtained by applying the rotation transform $\mathbf{V}(f)$ to $\mathbf{u_3}(f)$ as following:

$$\mathbf{N}(f) = \mathbf{V}(f)\mathbf{u_3}(f). \quad (27)$$

Because there are two possible solutions of $\mathbf{N}(f)$ as described in **2.1.3**, we need some methods to select a true one from them. If we know that the circle is on the ground and the camera is not set upside-down, then we can remove the inconsistent answer of $\mathbf{N}(f)$.

The tilt angle $\theta$ and the roll angle $\beta$ can be computed as following:

$$\left\{ \begin{array}{l} \theta = \frac{\pi}{2} - \cos^{-1} N_z(f) \\ \beta = \tan^{-1} \frac{N_x(f)}{N_y(f)} \end{array} \right. , \quad (28)$$

where $N_x(f)$, $N_y(f)$ and $N_z(f)$ are the $X$, $Y$ and $Z$ elements of $\mathbf{N}(f)$, respectively.

The translation vector $\mathbf{T}(\mathbf{f})$ can be obtained by applying the rotation transform $\mathbf{V}(f)$ to $\mathbf{C_0}(f)$ estimated with Eq.(22) as following:

$$\mathbf{T}(f) = \mathbf{V}(f)\mathbf{C_0}(f). \quad (29)$$

If an ellipse on the image plane has been detected and fitted, an oblique elliptical cone can be defined uniquely when the focal length $f$ is known. Then the extrinsic parameters can be computed from the oblique elliptical cone with the method described above.

In the case that the $f$ is unknown, the oblique elliptical cone whose apex is at the projection center and the base is the ellipse cannot be defined uniquely, but can be expressed as a function of the $f$. Thus the extrinsic parameters can be represented by functions of the $f$.

### 2.3 Calibration with unknown focal length

Here we describe an approach to calibrate the extrinsic camera parameters when the $f$ is unknown.

In order to obtain unique solution of the extrinsic parameters, we let the camera to observe two unconcentric co-planner circles. Let $\mathbf{Q_1}$ and $\mathbf{Q_2}$ are the two ellipses detected from the image. Assuming a focal length $f$, we can suppose two oblique elliptical cones. From them we can compute the unit vector of the ground. Let $\mathbf{N}_{ia}(f)$ and $\mathbf{N}_{ib}(f)$ be the two solutions estimated from $\mathbf{Q_i}; (i = 1, 2)$. Because the two circles are co-planar, the two vectors in one of the four pairs: $(\mathbf{N}_{1a}, \mathbf{N}_{2a})$, $(\mathbf{N}_{1a}, \mathbf{N}_{2b})$, $(\mathbf{N}_{1b}, \mathbf{N}_{2a})$ and $(\mathbf{N}_{1b}, \mathbf{N}_{2b})$ should be the same. However, if we assumed a wrong $f$, all the estimated normal vectors from $\mathbf{Q_i}; (i = 1, 2)$ will be different. Thus we can estimate the $f$ by minimum $E(f)$ given by

$$E(f) = \min(x_1, x_2, x_3, x_4), \quad (30)$$

where $x_1 = |\mathbf{N}_{1a}(f) \times \mathbf{N}_{2a}(f)|^2|$, $x_2 = \mathbf{N}_{1a}(f) \times$

$\mathbf{N}_{2b}(f)|^2$, $x_3 = |\mathbf{N}_{1b}(f) \times \mathbf{N}_{2a}(f)|^2$, $x_4 = |\mathbf{N}_{1b}(f) \times \mathbf{N}_{2b}(f)|^2$.

Once $f$ is determined, then the extrinsic camera parameters including the rotation parameters and the translation parameters can be computed uniquely.

## 3. Experimental Results

### 3.1 Simulation Results

In this simulation, we will use the world coordinate system and camera coordinates system as shown in figure 7. We assume that the length of an image sensor is $1/2$ inch, and the image resolution is $640 \times 480$ pixels. Therefore, the length of one pixel is $0.15875$ [mm].

Figure 8 shows ellipses synthesized with the parameter settings (called "*case-1*") of $f = 200$ [pixel], $\theta = 40$ [degree], $\beta = -10$ [degree], $Z_g = 3.0$ [m], and $r = 1.0$ [m].

Other examples of ellipses synthesized with the settings (called "*case-2*") of $f = 300$ [pixel], $\theta = 50$ [degree], $\beta = 30$ [degree], $Z_g = 3.0$ [m], and $r = 1.0$ [m].

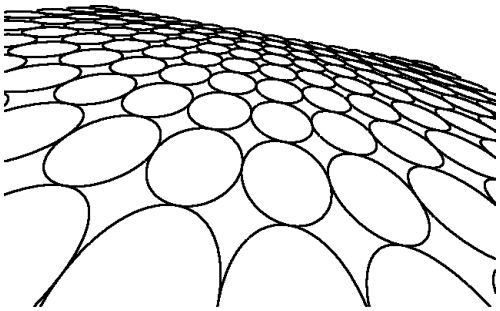

**Fig. 8** An example of ellipses synthesized by CG

#### 3.1.1 One circle

When $f$ is given, the extrinsic parameters can be estimated from a single circle. We have tested our method using ellipses in Figure 8 (*case-1*). 48 ellipses are selected as input data from the bottom to sixth lines. The resulted parameters are denoted by $\beta_1$ and $\theta_1$. 52 ellipses are selected from the top to the third line. The resulted parameters are denoted by $\beta_2$ and $\theta_2$. Also, the calibration result using 37 ellipses in *case-2* is denoted by $\beta_3$ and $\theta_3$.

The calibration results described above are summarized in Table 1. From these results, we can confirm that our method provides precise calibration results: In the cases of tiny reference ellipse (worst case), the RMS errors are less than $0.52$ and $0.13$ [degree] for $\beta$ and $\theta$ respectively. In the better case, it provides very accurate results of which the RMS errors for $\beta$ and $\theta$ are less than $0.09$ and $0.08$ [degree] respectively.

**Table 1** Some results by case of $f$ is known

| | RMS error | Standard deviation |
|---|---|---|
| $\beta_1$(degree) | 0.16 | 0.20 |
| $\theta_1$(degree) | 0.12 | 0.13 |
| $\beta_2$(degree) | 0.52 | 0.55 |
| $\theta_2$(degree) | 0.13 | 0.15 |
| $\beta_3$(degree) | 0.09 | 0.11 |
| $\theta_3$(degree) | 0.08 | 0.06 |

#### 3.1.2 Two circles

In the case of unknown $f$, our method calculates the extrinsic camera parameters and $f$ using a pair of projected ellipses. We have tested our method using 32 sets of the ellipse-pair randomly selected from the *case-1* and 17 sets from the *case-2*, respectively. The experimental results are summarized in Table 2 with suffixes 1 and 2.

From these results, our method can estimate accurate $f$ as well as other parameters.

**Table 2** Some results by case of $f$ is unknown

| | RMS error | Standard deviation |
|---|---|---|
| $f_1$(pixel) | 5.52 | 9.21 |
| $\beta_1$(degree) | 0.36 | 0.47 |
| $\theta_1$(degree) | 0.57 | 0.97 |
| $f_2$(pixel) | 7.19 | 11.89 |
| $\beta_2$(degree) | 0.11 | 0.15 |
| $\theta_2$(degree) | 0.51 | 0.85 |

#### 3.1.3 Comparison

In the case of $f = 200$ [pixel], $\theta = 38$ [degree] and $\beta = -10$ [degree], we synthesized a perspective projection image include a square whose length is $2.0$ [m] and it 's inscribed circle (Figure 9), and an orthographical projection image of the same scene. Using these images, we compared our method with the homography based approach.

**Fig. 9** An image for comparison with our method and homography method

Assuming that the correspondence between the four vertexes of the square on the two images has been established, we calculated the homography matrix, and then decomposed it into the rotation matrix, translation, and the surface normal vector

of the plane. The results are ($\theta_1 = 36.62$ [degree], $\beta_1 = 11.28$ [degree]) and ($\theta_2 = 38.11$ [degree], $\beta_2 = 9.71$ [degree] ). We determined that the latter result is valid, because it has smaller errors.

On the other hand, we applied our method to the same image. The result is $\theta = 37.94$ [degree] and $\beta = 10.22$ [degree].

The errors of four point correspondence are $0.11$ [degree] and $0.29$ [degree] for $\theta$ and $\beta$, respectively. Our method achieves smaller errors: $0.06$ [degree] and $0.22$ [degree] for $\theta$ and $\beta$, respectively.

We notice that the conditions of these calibrations are slightly different. That is, square based calibration requires four points correspondence data, while our method requires $f$ and a single image of a single circle but not point correspondence data.

If we regard the above conditions are balanced in some sense, we can claim that our method provides more precise results than four points correspondence calibration.

### 3.2 Experiments with real data

#### 3.2.1 Accquisition of an Environmental Map

Our calibration method has been implemented as an initialization procedure of a robot control system. Our system consists of a four wheel RC car with red and green LEDs, a fixed external camera (SONY DFW VL500), and a PC with a radio controller as shown in Figure 10 (a). In the system, the motion trajectory of the RC car is observed by detecting the LEDs from the images at video rate by the color target detector[15].

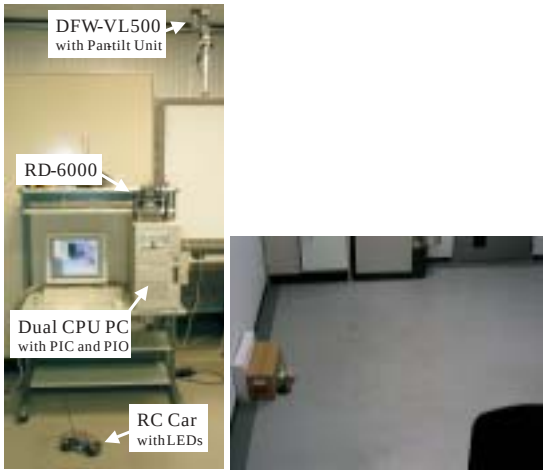


(a) System (b) Test environment

**Fig. 10** Experiment scenery

When the system is stared, it performs the camera calibration automatically. In this calibration, the RC car tries to move at low speed and keeping a constant steering angle. When the observed trajectory is closed, the system examines whether the trajectory is an ellipse or not. If the trajectory is an ellipse, the system performs the camera calibration. After this calibration, the robot trajectory in the image plane will be able to be transformed into the orthogonal view, i.e., we can monitor the real RC car movement in the scene. Figure 10 (b) shows a test environment.

Figure 11 (a) shows the robot trajectory when performing environment map generation using the robot body. That is, if we detected that the robot movement is blocked irrelevant to the action command, then we know that there must be an obstacle; if the LEDs disappeared from the image, then we know that there must be an occluding object hiding the robot from the camera view. In this way, we can generate the environment map. The resulted map is shown in figure 11 (b). Both of them are viewed from the virtual camera, and the real environment is showed in Figure 10 (b).

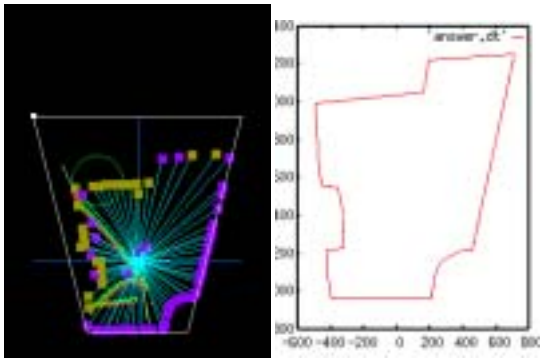

(a) (b)

**Fig. 11** (a) Some robot's move louses. (b) An obtained environmental map

#### 3.2.2 Accuracy Evaluation by other scenes

Our method is not limited to the camera calibration using a mobile robot. It can be applied to other scenes (see figure 12), e.g., manholes on flat roads, CD discs on a table, widening rings on the water surface, and so on.

## 4. Conclusion

This paper presented a new camera calibration method using circular pattern(s) drawn by four wheel robot. This approach can solve the problem estimating the extrinsic parameters between the camera and far flat objects.

Estimating homography matrix from point correspondence data suffers from the alternative decomposition problem. For solving this problem,

(a) Manholes on flat roads

(b) CD discs on a table

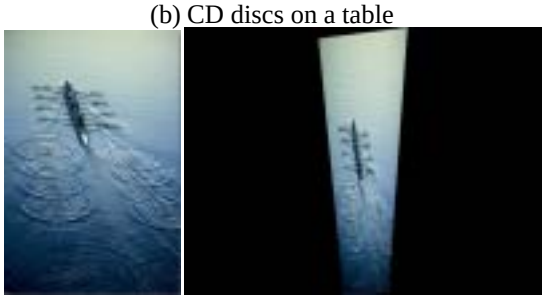

(c) widening rings on the water surface

**Fig. 12** Other scenes

two planar patterns or three cameras are used. Our method also produces dual solutions when referring a single circle. However, by referring two or more circles on same plane, our method produces a unique solution. This means that we can perform the camera calibration without adding planes or cameras.

In addition, we can realize an automatic camera calibration system based on our method. We will extend our method estimating image center and the radial distortion parameters in the future work.

**Acknowledgments:** This research was partially supported by the Ministry of Education, Science, Sports and Culture, Grant-in-Aid for Scientific Research (A), 12308016, 2000. The authors are grateful to associate professor T.Nakamura (Wakayama University) for helping the real robot experiments.

## References

1) O.Faugeras, “Three-Dimensional Computer Vision: A Geometric Viewpoint”, *MIT Press* , 1993.
2) X.Meng and Z.Hu, “A New Easy Camera Calibration Technique Based on Circular Points”, *Pattern Recognition* , Vol. 36, pp. 1155-1164, 2003.
3) G.Wang, F.Wu and Z.Hu, “Novel Approach to Circular Points Based Camera Calibration”,
4) J.S.Kim , H.W.Kim and I.S.Kweon, “A Camera Calibration Method using Concentric Circles for Vision Applications”, *ACCV* pp. 23–25, 2002.
5) Yang, C., Sun, F. Hu, Z.: “Planar Conic Based Camera Calibration”, *ICPR*, 2000.
6) Long, Q.: “Conic Reconstruction and Correspondence From Two Views”, *PAMI* , Vol.18, No.2, pp. 151–160, 1996.
7) S.Avidan and A.Shashua, “Trajectory Triangulation: 3D Reconstruction of Moving Points from a Monocular Image Sequence”, *PAMI* , Vol.22, No.4, pp. 348–357, 2000.
8) J.Heikkila and O.Silven, “A Four-step Camera Calibration Procedure with Implicit Image Correction”.
9) P.Sturm, “A Case Against Kruppa’s Equations for Camera Self-Calibration”, *PAMI* , Vol.22, No.10, pp. 348–357, 2000.
10) P.Gurdjos, A.Grouzil and R.Payrissat, “Another Way of Looking at Plane-Based Calibration: the Center Circle Constraint”, *ECCV* , 2002.
11) R.Sukthankar, R.Stockton and M.Mullin, “Smarter Presentations: Exploiting Homography in Camera-Projector Systems”, *ICCV* pp. 247-253, 2001.
12) R.J. Holt and A.N.Netravali, “Camera Calibration Problem: Some New Result”, *CVIU* , No.54, Vol.3, pp. 368–383, 1991.
13) P.Sturm and S.Maybank, “On Plane-Based Camera Calibration: A General Algorithm, Singularities, Applications”, *CVPR* , pp. 432–437, 1999.
14) H.Wu, T.Wada and Q.Chen, “ Robot Body Guided Camera Calibration”, *JPJS SIG Notes, 2003-CVIM-136*, pp. 67–74, 2003.
15) T.Wada, “Color-Target Detection Based on Nearest Neighbor Classifier: Example Based Classification and its Applications”, *JPJS SIG Notes, 2002-CVIM-134*, pp. 17–24, 2002.